2007

Fracture Logging of the AND-1B Core, McMurdo Ice Shelf Project, Antarctica

Terry J. Wilson
Ohio State University, wilson.43@osu.edu

T. Paulsen
University of Wisconsin - Oshkosh

A. L. Läufer
Bundesanstalt für Geowissenschaften und Rohstoffe (BGR)

C. Millan
Ohio State University

Terra Antartica
2007, **14**(3), 175-184

TERRA ANTARTICA
AN ANTARCTIC EARTH SCIENCE JOURNAL

Fracture Logging of the AND-1B Core, McMurdo Ice Shelf Project, Antarctica

T. WILSON[1]*, T. PAULSEN[2], A.L. LÄUFER[3] & C. MILLAN[1]

[1]School of Earth Sciences, Ohio State University, 125 South Oval Mall, Columbus, OH 43210 - USA
[2]Department of Geology, University of Wisconsin Oshkosh, 800 Algoma Boulevard, Oshkosh, WI 54901 - USA
[3]Bundesanstalt für Geowissenschaften und Rohstoffe (BGR), Stilleweg 2, 30655 Hannover - Germany
**Corresponding author* (wilson.43@osu.edu)

Abstract - Over 4300 natural and induced fractures were logged in AND-1B drill core. Induced fractures include steeply dipping, petal, petal-centreline, and core-edge induced fractures (n=421) which reach a maximum density of 5 fractures/metre. Subhorizontal induced extension fractures are also abundant. Natural fractures (n=1485) occur in Miocene to Pleistocene age strata and include faults, brecciated zones, veins and sedimentary intrusions. Kinematic indicators document dominant normal faulting, although reverse faults are also present. Vein types include slickenfiber veins along faults, opening-mode fibrous veins, pressure shadows on clast margins, and complex microvein webs within fault zones.

INTRODUCTION

The characterisation of fractures in drill core provides important information on the structural and tectonic evolution of rift basins. The type and orientation of natural fractures in cores and borehole walls, together with age constraints provided by dating the strata they cut, can be used to constrain faulting history and palaeostress directions associated with rifting in the western Ross Sea. Drilling-related fracturing, including borehole breakouts and tensile fractures in borehole walls and petal-centreline and disc fractures in core, provides a means to determine the orientations of the contemporary stresses in the crust surrounding the boreholes.

The Core Structure Measurements Group worked at the ANDRILL McMurdo Ice-Shelf Drill-Site Laboratory (Lab) and was responsible for obtaining core imagery and data needed to orientate the core to *in situ* coordinates, and for characterisation of natural and drilling-induced fractures in the core. Here we provide a summary of data acquired for core orientation and other applications, and an inventory of the fracture types documented by macroscopic logging of the AND-1B core.

METHODS

CORE ORIENTATION

Whole-Core Scanning

Whole-round core segments were scanned using the CoreScan II™ instrument manufactured by DMT, Germany. Segments up to 1 metre (m) in length were scanned by revolving the core on rollers as a digital line scanner traversed the length of the core. Scan resolution is 10 pixels/mm. A few selected core segments were scanned at 20 pixels/mm. Each whole-core scan file is named based on the depth in metres below seafloor (mbsf) of the top of the core segment. The PQ core obtained in core liners between the seafloor and 41.88 mbsf was not scanned. Poorly indurated or highly fractured intervals of core could not be scanned because they would not maintain their integrity on the rollers. We were able to obtain whole-core images of 56% of PQ3 core (between 41.88 and 283.04 mbsf), 89% of HQ core (between 238.04 and 702.64 mbsf), and 90% of NQ core (between 702.64 and 1284.87 mbsf). A table providing file names and depths of each whole-core scan entitled 'Whole Core Scans.pdf' is provided online at http://www.andrill.org. The whole-core scans can also be viewed in the Corelyzer core visualization application.

Intact Intervals of Core

Intact core intervals are continuous lengths of core where there has been no internal relative rotation of the core. Boundaries of these intervals are either breaks between core runs, where the core ends could not be fitted together, or are fractures within a core run where rotation occurred during coring (Fig. 1). In the PQ core, 29% of core runs could be fitted together end to end, and intact core intervals reached a maximum of 8.18 m in length. In the HQ core, 60% of the core runs could be fitted at their ends, and intact core intervals up to 39.21 m in length were found. In NQ core down to approximately 1068 mbsf, there were abundant fractures where the core 'spun' during coring, and intact intervals are short. Beneath this depth, NQ core integrity improved and intact intervals up to 54.38 m long were present. On site http://www.mna.it/english/Publications/TAP/terranta.html a table listing intact intervals of core (≥1 m in length) entitled 'Intact_Intervals_StratOrder.pdf' is available in the 'downloadable files' section.

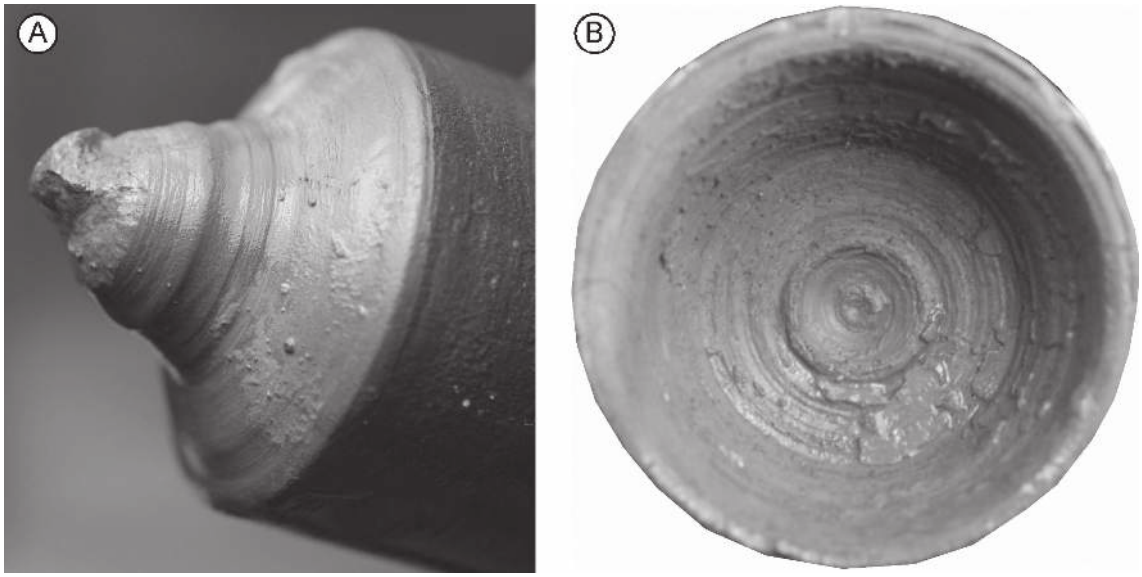

Fig. 1 – Photograph of subhorizontal fractures at 703.43 mbsf (A) and 735.27 mbsf (B) with circular 'potter's wheel' grooves documenting differential rotation of the core above and below. Core is 4.5 cm in diameter.

Core Orientation Procedure

A 'core reference frame' was defined by scribing a red line and a blue line (180° apart) along the length of each core run (Fig. 2A), using core splits with slots machined along their axis. Whole-core measurements were made with respect to the red line (designated core 'north'). The curatorial team split the core perpendicular to the scribe lines, with the red line placed down in the archive core split and the blue line placed down in the working core split. Core samples taken parallel or perpendicular to the slabbed core face preserve orientation with respect to the scribe lines. We note that, though care was taken in the core scribing process, deviation of the scribe lines from straight and 180° apart did occur where core was undersized (*i.e.* in the upper NQ core interval in particular) or where short, discontinuous core segments rotated in the scribing process. Red and blue lines may not have remained precisely 'down' in the core splits, and thus may not be perpendicular to the slabbed core face (Fig. 2B). Users requiring orientation should therefore measure the position of the scribe line relative to the slab face to assure correct orientation.

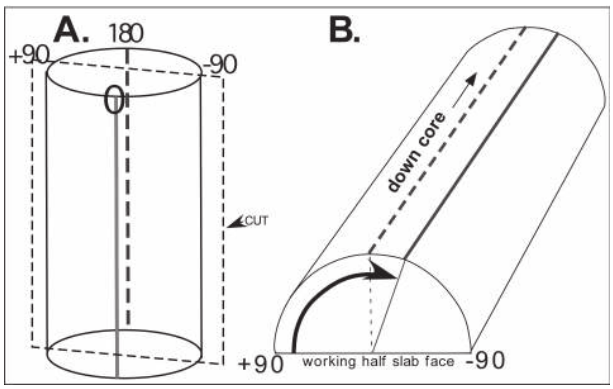

Fig. 2 – Core reference frame used for core measurements and orientation. The red scribe (solid line marked '0') line is designated as arbitrary 'north' and the blue scribe line (dashed line marked '180') is drawn 180° opposite (A). The core is cut perpendicular to these lines, and the blue scribe line is placed down in the working half of the core. Although the blue scribe line should be 90° from the slab face of the working half of the core (B), it is important to measure the true position of the line when taking oriented samples, as various procedural problems may have caused misalignment.

Whole-core images will be digitally 'stitched' together into complete intact core intervals during off-ice work. These intact core intervals will be compared to equivalent depth intervals of magnetically oriented borehole televiewer (BHTV) imagery of the borehole walls to locate the same features (*e.g.* fracture planes, bedding planes, large lonestone clasts) in both images. If matching features are identified, an average 'rotation angle' to match the position of core features to the oriented BHTV image will be computed for each intact core interval. This rotation angle can then be used to reorientate measurements or samples made with respect to the scribe lines into their correct *in situ* position when the core was in the ground (see Paulsen et al. 2002). Alternate means of core orientation, required in particular for core intervals where no borehole-wall imagery was acquired, will include structural dip direction and steep drilling-induced fractures, if these features prove to have uniform orientations.

FRACTURE LOGGING METHODS

Fracture logging was carried out at the Drill Site Lab on the whole core. The depth of the top and bottom of each fracture was recorded in metres below seafloor. Fracture dip and dip direction were measured relative to the core axis and the red scribe line, respectively. Macroscopic observations of fracture surface features (where open) and of fracture fill types and textures were made to assess shear or extensional mode of fracture origin and to determine displacement sense and magnitude. Core structures were documented with digital photographs and samples were taken for

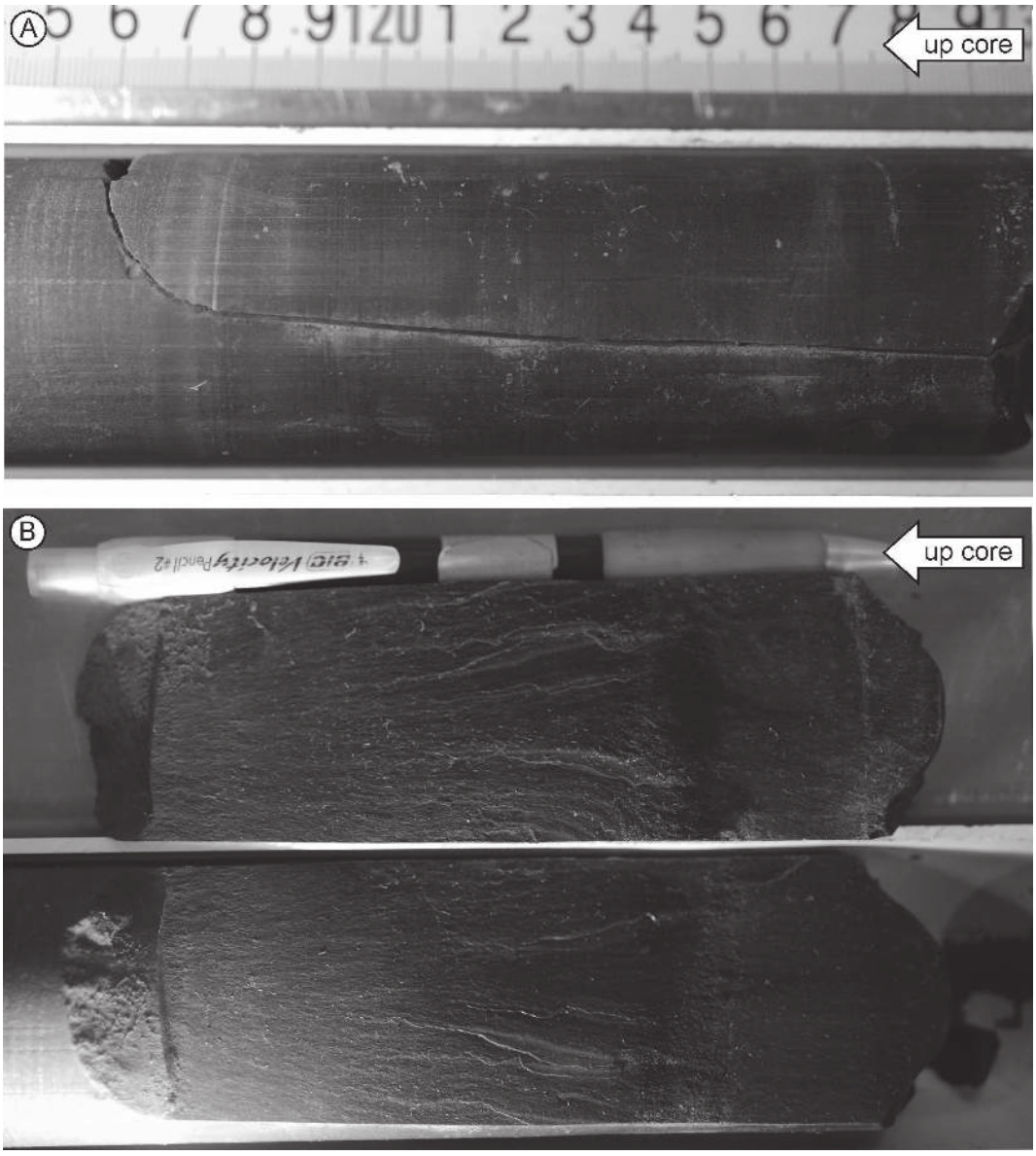

Fig. 3 – Photograph of petal-centreline fracture in the AND-1B core at 728.16 mbsf. Note petal curvature inward and downward from the margin and vertical centreline fracture following core axis (A), and hackle plume surface structure documenting downcore propagation (B). Core is 4.5 cm in diameter and *c.* 16 cm long.

microscopic characterisation. Over 4300 fractures of all types were logged in the AND-1B core.

RESULTS

INDUCED FRACTURES IN THE AND-1B CORE

Fractures that form during drilling (*i.e.* in the rock around the drill bit), coring (*i.e.* on entry or in the core barrel), or subsequent handling of the core are classed as 'induced' fractures.

Petal, Petal-Centreline, and Core-Edge Fractures

Petal, petal-centreline (Fig. 3), and core-edge fractures consist of steeply dipping, typically curviplanar, extension fractures that propagate in the formation below the drill bit and then are partially captured in the core as drilling proceeds. Fractographic features, including arrest lines and fine hackle plumes, demonstrate propagation of these fractures inward and downward along the core axis (Fig. 3). The orientation of these fracture planes parallels the maximum horizontal stress in the crust and is perpendicular to the minimum horizontal stress (Lorenz et al. 1990). Once the core is oriented, we will be able to define horizontal stress orientations at the MIS site from the steep drilling-induced fracture set.

The distribution of the 410 petal, petal-centreline, and core-edge fractures we identified is compiled in figure 4. The density of these fractures reaches up to *c.* 5 fractures/metre, but averages 0.33 fractures/metre over the entire length of core. Petal-centreline fractures and core-edge fractures occurred most commonly at or near the top of core runs, but also were present mid-run and, more rarely, near the base of runs. Petal, petal-centreline, and core-edge fractures are most abundant in mudstones, which

commonly were more difficult to drill and were associated with higher pump pressures during drilling, and are uncommon in the diatomites and diamictite lithologies.

Subhorizontal Drilling-, Coring-, and Handling-Induced Fractures

Subhorizontal induced fractures of several types occur through the AND-1B core. Fractures along which the core has rotated are identified by the presence of circular grooves and/or by their conical shape (Figs. 1A & 1B). These form as core rotates below or within the core barrel, and define breaks between continuous, intact core intervals. Subhorizontal extension fractures can form when the core is broken off at the end of a run, when the rock is released from load upon entering the core barrel, during flexing of the core splits during transport, or due to handling during core processing. Surface fractographic features demonstrate opening of the fractures due to tension. Hackle plume structures were common on these fractures in some core lithologies (Fig. 5A). Unusual arrays of conchoidal arrest lines, marking pauses in fracture propagation, were common in fine-grained lithologies in the core (Fig. 5B). These induced fractures also provide constraints on the *in situ* stress regime (*e.g.* Li & Schmitt 1997).

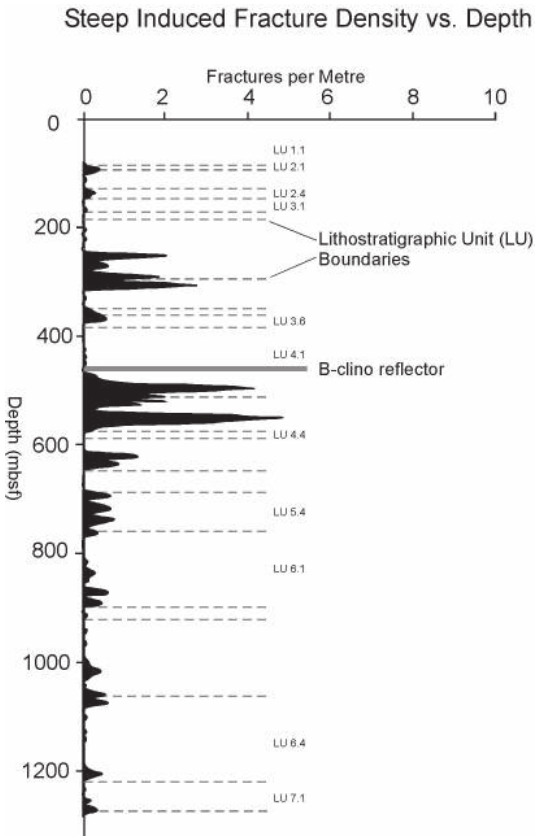

Fig. 4 – Fracture density plot showing the number of petal, petal-centreline, and core-edge fractures per metre of core with relation of depth within the AND-1B core.

NATURAL FRACTURES IN THE AND-1B CORE

'Natural' fractures are pre-existing fractures in the rock that are intersected by coring. Natural fractures are identified based on their geometry and characteristics, such as truncation/offset of bedding, mineralization or brecciation. The distribution of the 1475 natural fractures identified in the core is compiled and compared to core lithology in figure 6. Fracture densities up to *c.* 6 fractures/metre occur both in the upper and lower portions of the core. Overall, the average fracture density is 1.2 fractures/metre. Natural fractures are present in the highest core that we were able to log (*i.e.* not retrieved in plastic liners), with conjugate faults occurring at 42.35 mbsf. There is a zone of high fracture density between *c.* 125 and 300 mbsf, within an interval currently estimated to range in age between approximately 1 and 3 Ma. Natural fractures are consistently present through the core below *c.* 450 mbsf, the estimated depth of the 'B-clino' seismic reflector. This is consistent with the presence of seismically detectable faults below this horizon. Overall the natural fracture record shows that deformation of the sedimentary sequence continued to a young age, into the Pleistocene. These structures will provide information on the palaeostress and strain regime associated with deposition of the Neogene strata, including deformation within the Terror Rift.

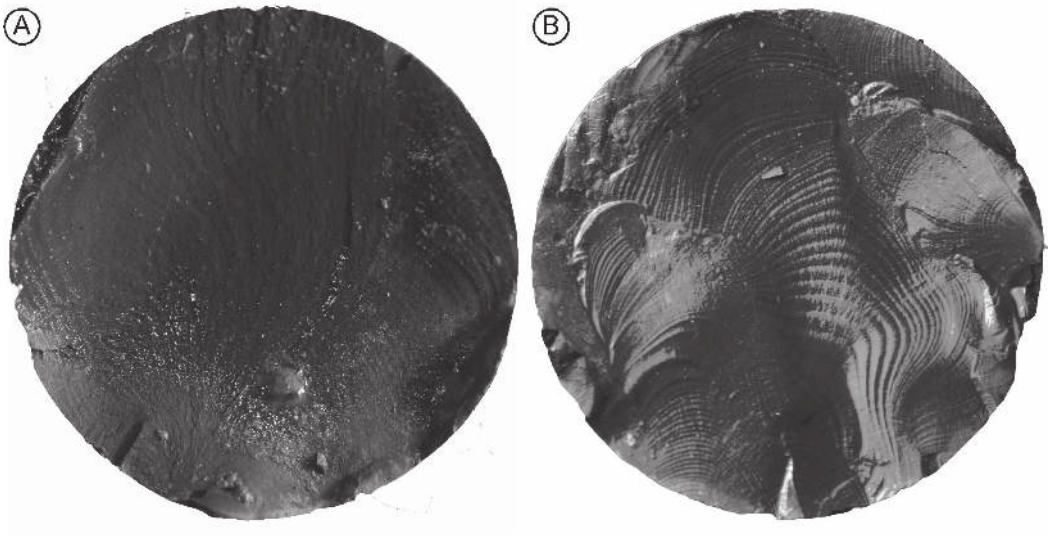

Fig. 5 – Photograph of subhorizontal fractures at 756.44 mbsf (A) and 746.05 mbsf (B) in the AND-1B core. Hackle plume (A) and conchoidal arrest lines (B) demonstrate induced, tensile fracture origin. Core is 4.5 cm in diameter.

Faults

Open fractures with highly polished, slickensided and striated surfaces (Fig. 7) are common throughout the core and occur in all lithologies, but are particularly abundant in mudrock intervals. Closed fractures appearing as dark millimetre-scale bands are probably slickensided faults, because many truncate bedding and some opened during handling to reveal surface striae and, in some cases, surface mineralization. Many faults have thin patches of vein material forming slickenfiber steps that define the sense of displacement (Fig. 8). Other faults have been completely filled by vein material, discussed below. Mineralization along faults includes calcite, a dark green mineral that is most likely chlorite, pyrite, and some unidentified minerals. Almost all faults have striae parallel or close to the dip direction; oblique slip lineations deviating more than 20° from the dip direction are very rare. Faults with surface kinematic indicators all had normal-sense shear displacement.

Faults observed to offset bedding typically have offset magnitudes of a few millimetres up to 3 cm. Some breccia zones and zones of dense faulting and/or veining in the core could mark faults with larger-magnitude displacement, but it is not possible to detect large offset magnitude in the core. Most faults that displace bedding have normal-sense dip separation, but a subset have reverse-sense shear (Fig. 9). Locally, reverse and normal faults are found in close proximity, even in adjacent beds (Fig. 10). These instances suggest a complex strain field, perhaps associated with deformation due to glacial overriding. The majority of faults in the core, however, have normal-sense displacement, 50°-70° dip angles and commonly have conjugate geometries, as expected for tectonic deformation in a rift regime. In a few cases, faults with millimetre-scale offset of bedding die out upcore or downcore without

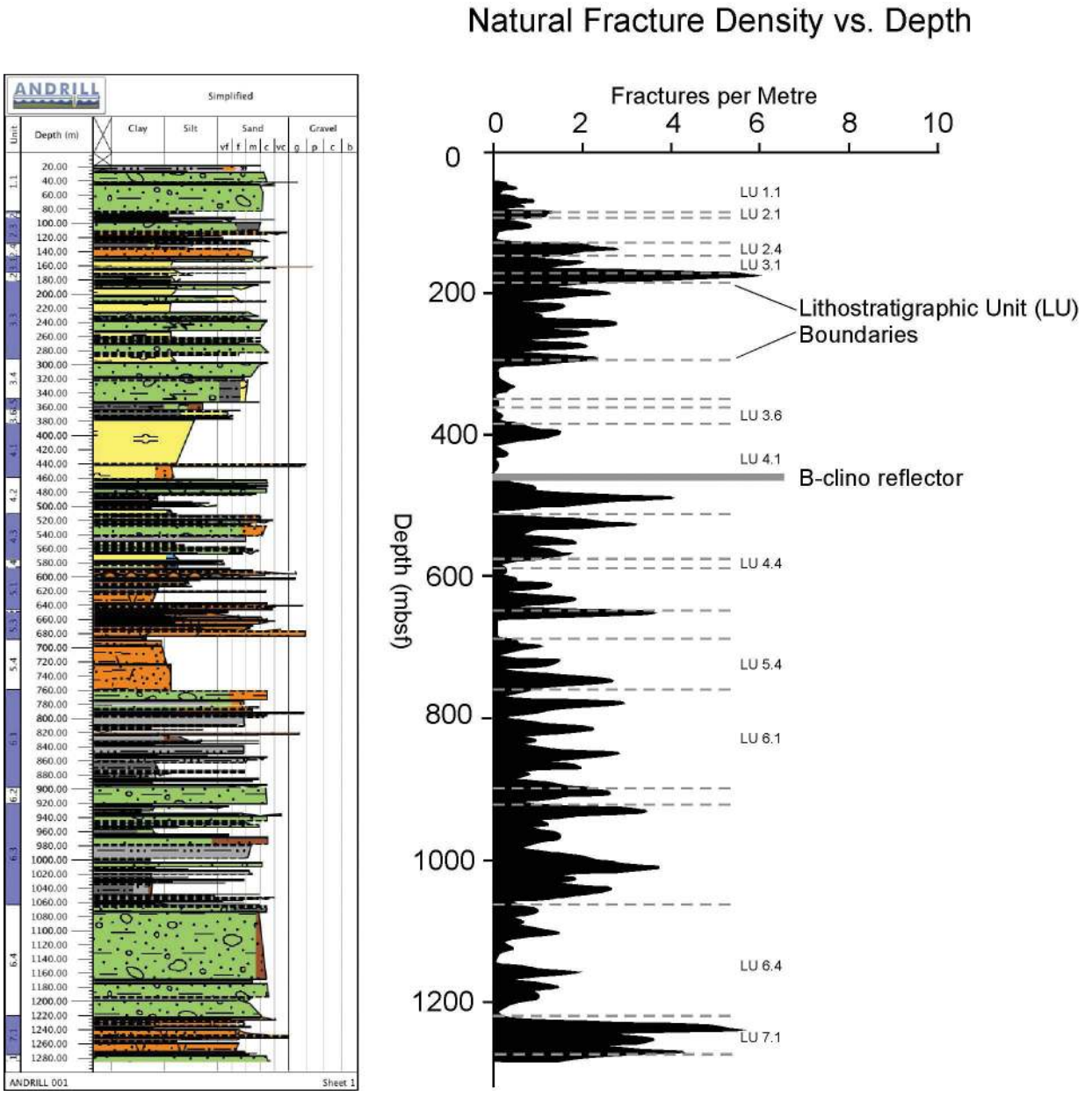

Fig. 6 – Fracture density plot showing the number of natural fractures (faults and veins) per metre of core with relation to depth, lithology, and lithostratigraphic unit boundaries within the AND-1B core.

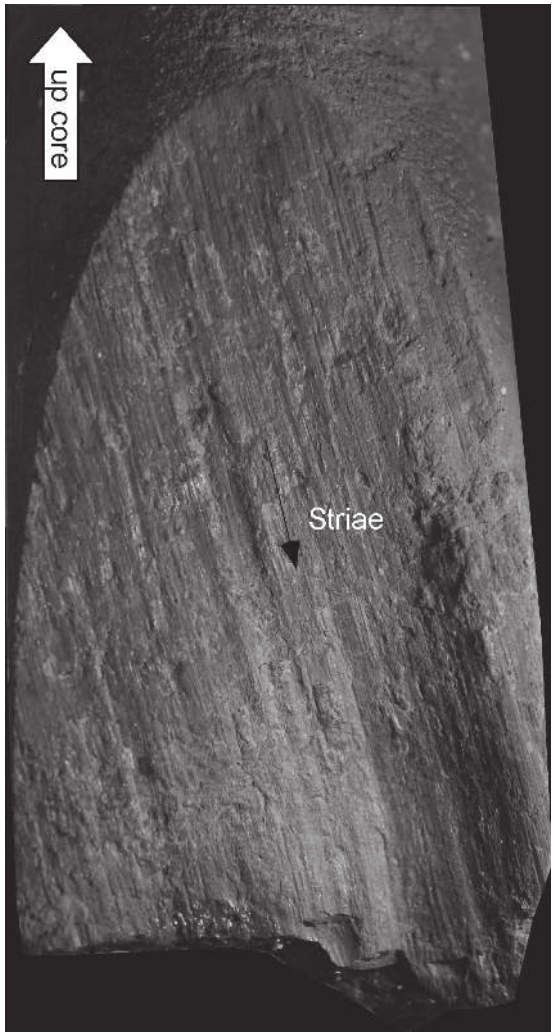

Fig. 7 – Photograph of a high-angle normal fault with down-dip striae in the AND-1B core at 1086.25 mbsf. Core is 4.5 cm in diameter.

displacing bedding above or below, characteristic of faulting penecontemporaneous with deposition. Locally, cataclastic zones occur at the base of clasts, and compaction faults extend downward from the base of clasts, also suggesting faulting occurred, at least in part, penecontemporaneous with deposition. These penecontemporaneous structures have the same mineralization as tectonic faults. Discrimination between tectonic and glaciotectonic faulting will be a focus for further study.

Fig. 8 – Photograph of a striated fault surface with fibrous calcite steps defining normal-sense movement at 904.28 mbsf in the AND-1B core. Core is 4.5 cm in diameter. Arrow points upcore.

Breccias

Breccias of at least two distinct types occur in the AND-1B core. Brecciation involving injection of remobilized sedimentary matrix produces a 'jigsaw' breccia where clasts can be fitted together. Injection both along and at high angles to bedding planes operated to form the breccia texture (Fig. 11). Elsewhere, zones or discontinuous pockets of calcite-cemented breccia occur along planes that are likely faults (Fig. 12).

Veins

Veins are very abundant in the AND-1B core. Vein thickness ranges from <1 mm to 2 cm, and veins commonly contain fibres, either perpendicular or parallel to vein margins. Where veins cut massive volcanic rocks and clasts, the veins and/or voids along the veins are

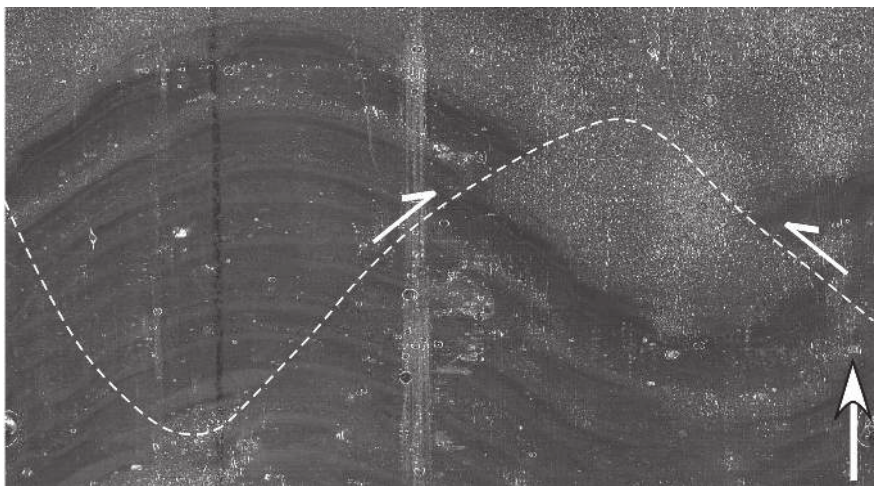

Fig. 9 – Whole-round CoreScan II™ image of a reverse fault offsetting bedding at 1024.19 mbsf in the AND-1B core. Core is 4.5 cm in diameter. Arrow points upcore.

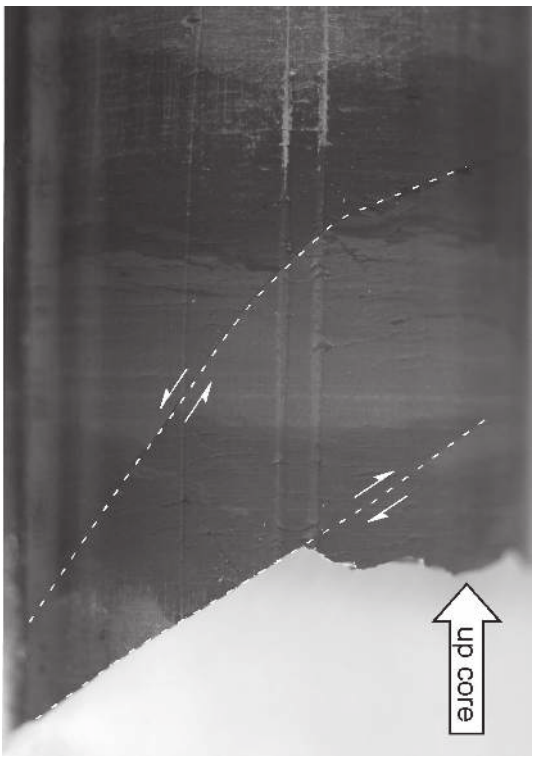

Fig. 10 – Photograph of a reverse and normal fault in adjacent beds at 1071.76 mbsf in the AND-1B core. Core is 4.5 cm in diameter.

Fig. 11 – Whole-round CoreScan II™ image of a 'jigsaw' breccia with clastic injections both across and along bedding at 1233.56 mbsf in the AND-1B core. Core is 4.5 cm in diameter.

filled by euhedral crystals, indicating growth into open void space. Vein fill minerals include calcite, pyrite, a dark green mineral (chlorite?), and some unidentified dodecahedral and needle-shaped crystals that are likely zeolites. The abundance and pervasive distribution of veins indicate abundant fluids, substantial pore pressures, and a strong role of fluids in deformation of the strata.

Many veins are clearly associated with fault planes. Attributes of veins interpreted as faults include dips between 55° and 75°, typical of fault planes, conjugate geometries typical of normal faults (Figs. 13 & 14), precipitation in steps or pull-aparts along fault surfaces (Fig. 15), arrangement in *en echelon* arrays defining normal-displacement shear zones, and occurrence along planes that have slickensided host rock surfaces. Complex 'webs' of veins occur, typically branching from planar veins that are likely fault planes (Fig. 16). Commonly both larger and hairline veins in the webs have conjugate geometries, again suggesting that these vein complexes represent fault zones. The diffuse, pervasive nature of the veining suggests that tensile strength of the rocks was low and fluid pressures were high.

Remarkably (for a vertical core), there are large numbers of very steeply dipping (>75°) calcite veins in the lower portion of the core, some over 1 m long. The steep veins are typically microfolded (Fig. 17), indicating that the veins formed early, when rocks were cohesive enough to crack but not fully lithified, and then were shortened by buckling as the surrounding, less competent host rocks compacted. Vertical fibrous calcite veins also occur as pressure

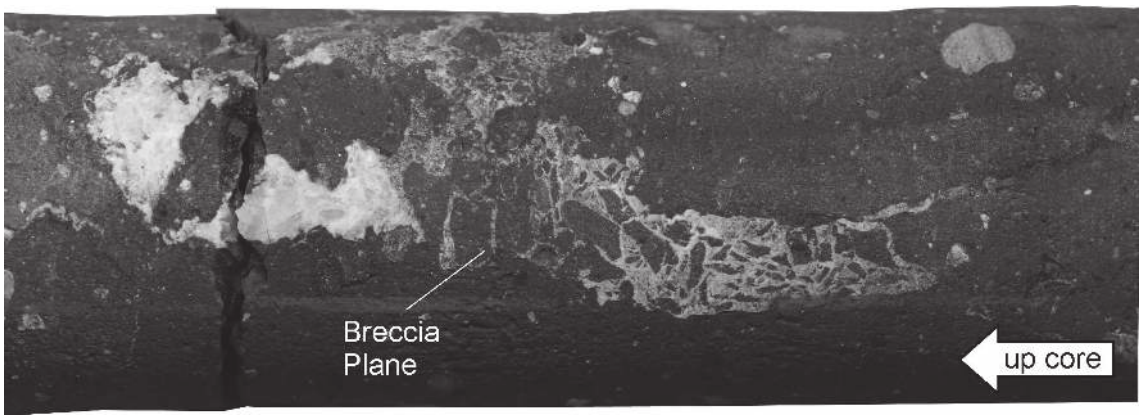

Fig. 12 – Photograph of a planar zone of calcite-cemented breccia at 1279.21 mbsf in the AND-1B core. Core is 4.5 cm in diameter.

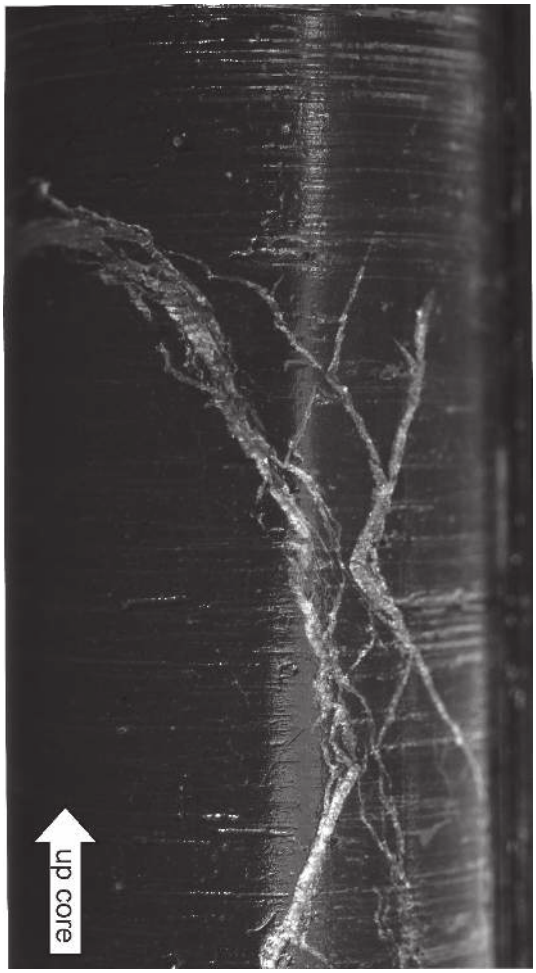

Fig. 13 – Photograph of calcite veins with a conjugate geometry and dips typical of normal faults (55° to 70°) at 961.26 mbsf in the AND-1B core. Core is 4.5 cm in diameter.

shadows on the margins of pebbles (Fig. 18), further suggesting the veins developed during vertical loading and compaction. Arrays of short (1-2 cm length), vertical veins are also microfolded (Fig. 19A) and, in profile, form radiating patterns reminiscent of mud cracks (Fig. 19B). These may represent arrays of syneresis cracks, formed during dewatering of the sedimentary section. In rare instances, veins have ladder geometries where they follow bedding and then ramp up and cut across bedding to successively higher horizons where they again parallel bedding. This ladder geometry suggests 'natural hydrofracturing' under high fluid pressures.

Sedimentary Intrusions

Several examples of sandstone dikes intruding downward along fractures from the base of beds were observed (Fig. 20). Some of these dikes also had margins of calcite and/or the dark green mineral commonly observed on fault surfaces. Many closed fractures with steep dips typical of fault planes were filled with granular material of either clastic or cataclastic origin. Microscopic analysis will reveal whether these are also sedimentary intrusions. There were some intervals of brecciated core where remobilized sedimentary matrix intruded into coherent blocks in a 'ladder' pattern, injecting along

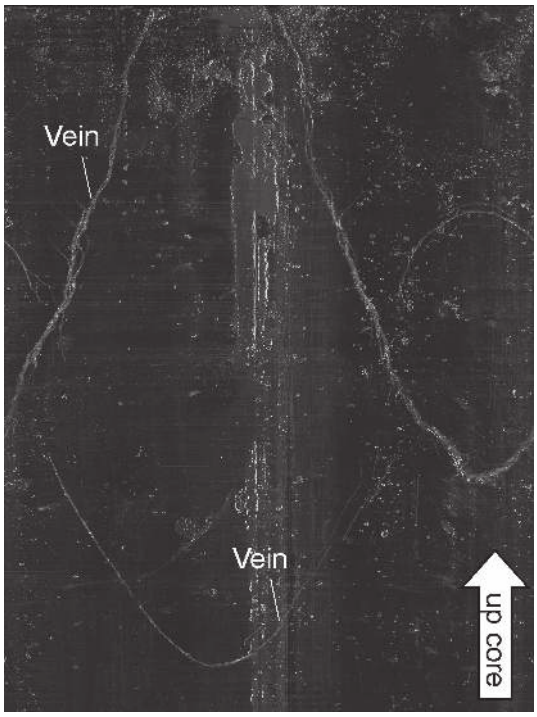

Fig. 14 – Whole-round CoreScan II™ image of calcite veins with a conjugate geometry typical of normal faults at 1036.08 mbsf in the AND-1B core. Core is 4.5 cm in diameter.

short, steep fractures connecting bedding-plane-parallel 'sills'. The presence of discrete sedimentary dikes and intrusion of clastic material in breccia zones shows that deformation of the sequence was occurring prior to complete lithification of the strata. The association with the same vein material seen on fractures throughout the core implies that much or all of the faulting and veining may be pre-lithification in age.

Fig. 15 – Photograph of calcite-filled pull-aparts indicating normal-sense fault displacement at 1173.62 mbsf in the AND-1B core. Core is 4.5 cm in diameter. Arrow points upcore.

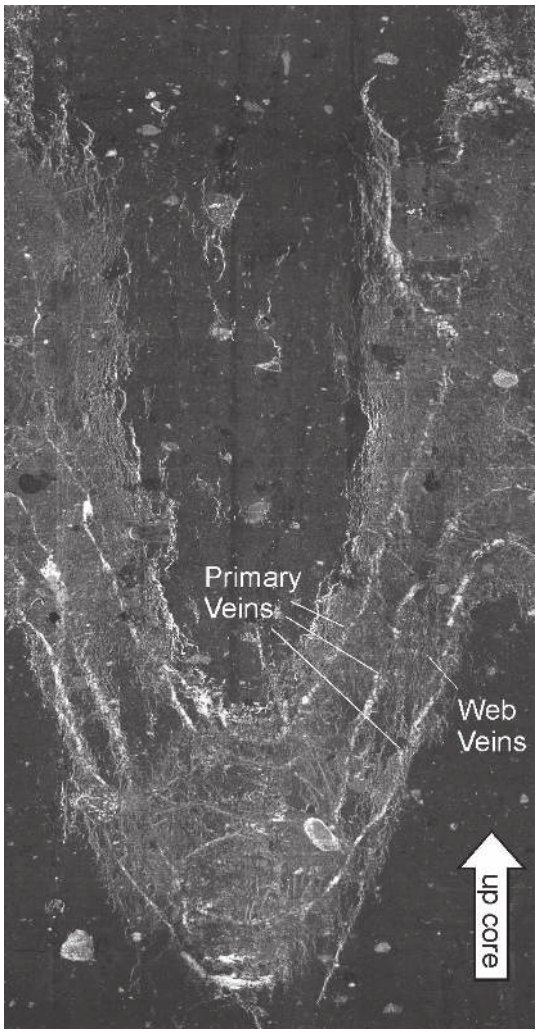

Fig. 16 – Whole-round CoreScan II™ image of a web of hairline calcite veins connecting several well-developed calcite veins (faults) at 1005 mbsf in the AND-1B core. Core is 4.5 cm in diameter.

Fig. 17 – Photograph of folded, steeply dipping calcite vein at 1114.76 mbsf in the AND-1B core. Core is 4.5 cm in diameter. Arrow points upcore.

DISCUSSION

Both natural and drilling-induced fractures are abundant in AND-1B drill core. The most significant drilling-induced fractures are the abundant, steeply dipping petal, petal-centreline, and core-edge fractures. These induced fractures will provide a record of the *in situ* stress orientations in the crust surrounding the borehole, once the core has been oriented. The most abundant natural fractures in the AND-1B core are normal faults and various types of calcite veins. There are also some reverse faults, brecciated zones, and sedimentary intrusions in the core. The presence of sedimentary intrusions and the abundance of veining documents high fluid pressures during deformation. The sedimentary intrusions and steep veins folded by compaction indicate that deformation occurred prior to complete lithification of the strata, suggesting deformation was approximately coeval with deposition. The large population of natural fractures (≥1475), occurring in core strata from Miocene to Pleistocene in age, indicates that deformation has affected this sector of the basin throughout deposition of the strata. After the core fractures have been oriented, comparison of their trends with seismically mapped faults will help determine if the deformation is related to evolution of the Terror Rift, which seems likely given the dominance of normal faults in the core. This analysis, together with detailed correlation of the depth distribution of deformed intervals of the core with respect to episodes of glacial advance and retreat documented from the core strata, will help discriminate glaciotectonic and tectonic deformation. The abundant fractures in the AND-1B core will provide a detailed history of Neogene deformation of strata in the McMurdo Ice Shelf region, including palaeostress and contemporary stresses driving the deformation.

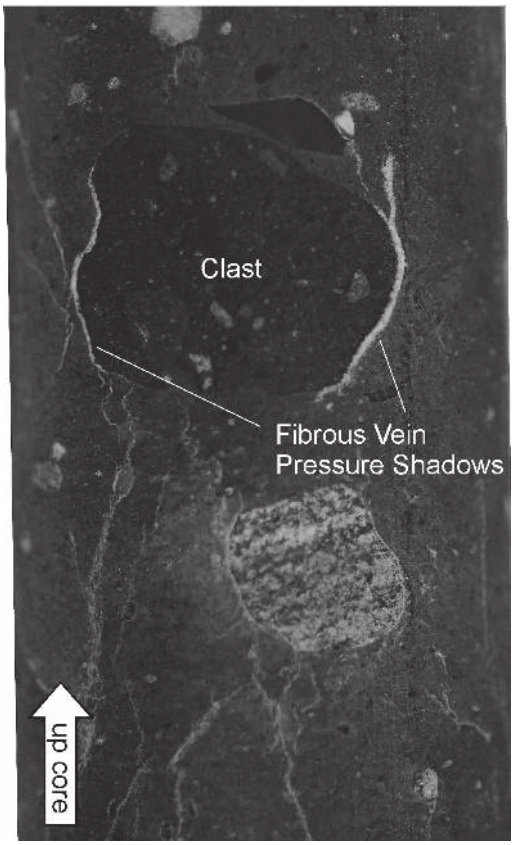

Fig. 18 – Photograph of fibrous calcite pressure shadows on the margin of a pebble at 943.87 mbsf in the AND-1B core. Core is 4.5 cm in diameter.

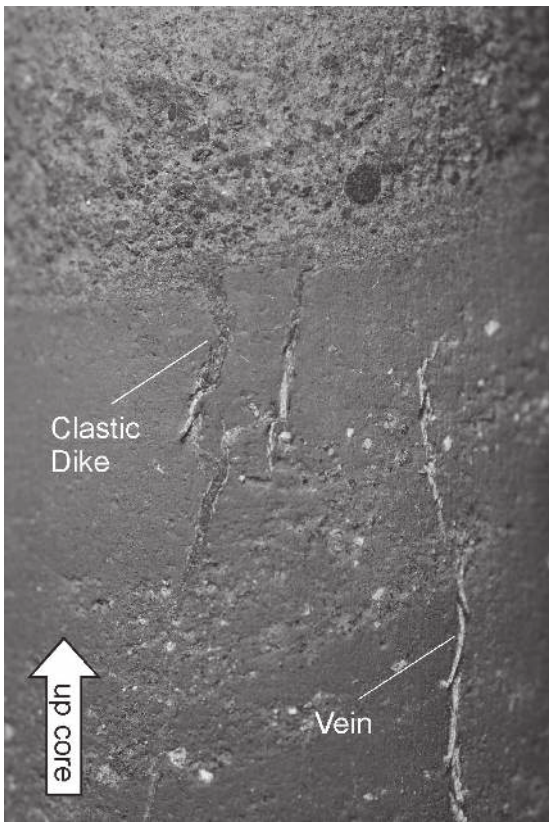

Fig. 20 – Photograph of a sandstone clastic dike intruded downwards into a finer grained horizon and a proximal calcite vein with similar orientation at 1050.38 mbsf in AND-1B core. Core is 4.5 cm in diameter.

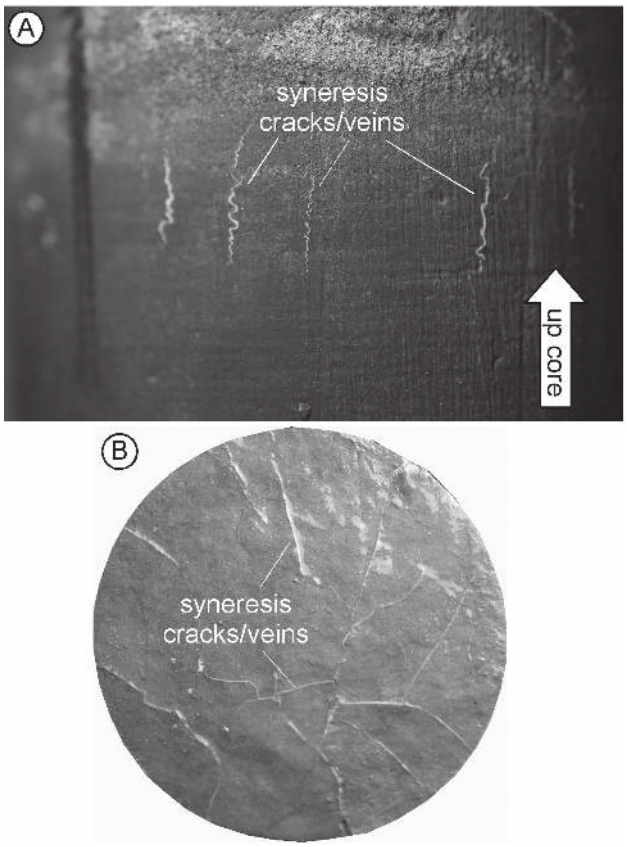

Fig. 19 – Photograph of short, folded vertical calcite veins (A) that radiate in horizontal cross section (B) at 1234.87 mbsf in the AND-1B core. These veins resemble syneresis cracks formed during dewatering. Core is 4.5 cm in diameter.

Acknowledgements – The ANDRILL project is a multinational collaboration between the Antarctic programmes of Germany, Italy, New Zealand and the United States. Antarctica New Zealand is the project operator and developed the drilling system in collaboration with Alex Pyne at Victoria University of Wellington and Webster Drilling and Enterprises Ltd. Antarctica New Zealand supported the drilling team at Scott Base; Raytheon Polar Services Corporation supported the science team at McMurdo Station and the Crary Science and Engineering Laboratory. The ANDRILL Science Management Office at the University of Nebraska-Lincoln provided science planning and operational support. Scientific studies are jointly supported by the US National Science Foundation, NZ Foundation for Research, Science and Technology and the Royal Society of NZ Marsden Fund, the Italian Antarctic Research Programme, the German Research Foundation (DFG) and the Alfred Wegener Institute for Polar and Marine Research.

REFERENCES

Li Y. & Schmitt D., 1997. Well-Bore Bottom Stress Concentration and Induced Core Fractures. *Amer. Assoc. of Petrol. Geol. Bull.,* **81**, 1909–1925.

Lorenz J.C., Finely S.J., & Warpinski N.R., 1990. Significance of Coring Induced Fractures in the Mesaverde Core, Northwestern Colorado. *Amer. Assoc. of Petrol. Geol. Bull.*, **74**, 1017–1029.

Paulsen T.S., Jarrard R.D. & Wilson, T.J., 2002. A Simple Method for Orienting Drill Core by Correlating Features in Whole-Core Scans and Oriented Borehole Wall Imagery. *J. of Struc. Geol.*, **24**, 1233–1238.